A Neutron Reflectivity Investigation of Surface and Interface Segregation of Polymer Functional End Groups

J. F. Elman,[†,‡] B. D. Johs,[§] T. E. Long,[‡,∥] and J. T. Koberstein[*,†]

Institute of Materials Science and Department of Chemical Engineering, University of Connecticut, Storrs, Connecticut 06269-3136, Analytical Technology Division and Corporate Research Labs, Eastman Kodak Company, Rochester, New York 14650-2136, and J. A. Woollam Company, Lincoln, Nebraska 68508

Received January 18, 1994; Revised Manuscript Received June 28, 1994[⊗]

ABSTRACT: The distribution of polymer terminal groups at surfaces and interfaces is assessed by neutron reflectometry (NR) experiments on end-functional polystyrenes. Mono-terminated polystyrenes (PS) are synthesized anionically to include a short perdeuteriostyrene sequence adjacent to the end groups for the purpose of selective contrast labeling of the end groups for NR. The location of deuterium serves as a marker to indicate the location of the adjacent end group. Three cases of end group surface segregation are examined: a "neutral" control specimen prepared by proton termination, a "repulsive" end group system terminated with high surface energy carboxylic acid end groups, and an "attractive" end group system containing low surface energy fluorocarbon chain ends. All three systems exhibit damped oscillatory end group concentration depth profiles at both the air and substrate interfaces. The periods of these oscillations correspond approximately to the polymer chain dimensions. The surface structure of the "control" sample is dominated by the *sec*-butyl initiator fragment located at one end of the chain. This end group has a lower surface energy than that of the PS backbone and segregates preferentially to both the air and substrate interfaces. In the fluorosilane-terminated material, the low energy fluorinated end groups are depleted from the substrate interface but are found in excess at the air interface. In the carboxy-terminated material, the high energy carboxyl end group segregates preferentially to the silicon oxide overlayer on the substrate and is depleted at the air surface. X-ray photoelectron spectroscopy (XPS) is utilized to provide complementary characterization of the atomic surface compositions for the three systems.

Introduction

The surface and interfacial properties of multicomponent polymer systems can be radically different from those of the bulk and may be dominated by even small amounts of chemical species that adsorb preferentially at the interface.[1] Interfacial segregation effects of this nature are of obvious fundamental interest and are often of critical importance to applications requiring quantitative control of the surface properties of multicomponent polymers. Surface segregation phenomena have been observed in virtually all multicomponent polymer mixtures, including blends,[2,3] solutions,[4] and block copolymers.[5] The fundamental driving force governing this behavior is the difference in surface energy between the mixture components. The ultimate surface structure is defined by a balance of the surface energy gain due to segregation and the chemical potential energy loss as a result of the demixing required to form the surface composition gradient.[6] In certain cases, the balance may be subject to entropic constraints such as the chemical bond joining unlike sequences in a diblock copolymer.

We have recently been interested in interfacial segregation phenomena for end-functional homopolymers, where the intentional addition of functional termini onto polymer chains can profoundly influence their surface and interfacial properties.[7-12] Of particular interest were surface tension measurements[7] on α,ω-functionally terminated poly(dimethylsiloxane)s, that suggested that low (i.e., relative to that of the chain backbone) surface energy methyl chain termini were selectively adsorbed at the polymer–air interface while high relative surface energy amine end groups were depleted from the surface. Lattice model calculations[8] are found to be in reasonable agreement with the experimental surface tension data and also predict surface depletion for amine end groups and surface adsorption for methyl end groups. X-ray photoelectron spectroscopy (XPS) measurements[9] confirmed the depletion of amine end groups at the surface, but a technique was not available to investigate the surface segregation of the low energy methyl end groups.

Theoretical calculations considering the chain conformation of polymer melts confined between two plates[13] and our own lattice model calculations[8] predict that surface end group composition profiles must be oscillatory in nature, due to the connectivity between the end group and the chain backbone. The composition of end groups integrated over one polymer chain length must equal the bulk end group composition. Therefore, any adsorption layer must necessarily be followed by a depletion layer, and vice versa. Angle dependent XPS measurements of end group composition depth profiles[9] were found to be inconsistent with simple monotonic decay functions, but the precision of the data was insufficient to prove that the profiles were of an oscillatory nature. The reproducibility of these data was poor due to several factors including the inherently broad distribution in molecular weight of the materials, the low concentration of end groups, and the low photoelectron yield for the nitrogen atoms in the end group.

In this paper, we report the results of a neutron reflectivity (NR) study of the end group distributions at polymer melt surfaces and interfaces. The use of this technique circumvents some of the problems encountered in our previous investigation. The study of the polymer chain end distribution at a surface has been attempted previously by NR measurements;[14] however the model profiles employed for analysis of the neutron reflectivity curves did not properly account for the connectivity of

* To whom correspondence should be addressed.
† University of Connecticut.
‡ Eastman Kodak Co.
§ J. A. Woollam Co.
∥ Present address: Eastman Chemicals Co., Kingsport, TN.
⊗ Abstract published in *Advance ACS Abstracts,* August 1, 1994.

0024-9297/94/2227-5341$04.50/0

Table 1. SEC Characterization Results

end group	M_n	M_w/M_n	M_n of end group
proton	10 300	1.07	1
fluorosilane	10 900	1.06	405
carboxy	10 600	1.06	44

chain end and backbone, as discussed above. The present study utilizes anionically synthesized end-functional diblocks, poly[*sec*-butyl-*b*-styrene-*b*-perdeuteriostyrene-*b*-end group], where the short deuterated block is terminated by one of three different end groups: a low energy fluorosilane, a neutral hydrogen, or a high energy carboxyl group. These materials have a narrow molecular weight distribution and provide a strong contrast for location of the end group, and the contrast is independent of the end group type. NR analysis is employed to characterize the spatial distribution of deuterium, which reflects the distribution of the adjacent chain end, at both the air–polymer and substrate–polymer interfaces. Complementary analysis by XPS is performed when possible to corroborate these measurements.

Experimental Section

Materials and Purification. Cyclohexane (Aldrich) was stirred in the presence of sulfuric acid for 10 days in order to remove any unsaturated impurities. The solvent was decanted from the acidic layer and distilled under nitrogen from a sodium dispersion immediately prior to polymerization. Tetrahydrofuran (Fisher) was distilled twice from sodium/benzophenone under nitrogen and vacuum distilled immediately prior to use. Styrene (Aldrich) was stirred over finely crushed calcium hydride for 24 h. The monomer was degassed several times by the freeze–thaw method and vacuum distilled. The monomer was stored at −25 °C until further use. Immediately prior to polymerization, the monomer was vacuum distilled from dibutylmagnesium (DBM), which efficiently removes any residual traces of water and oxygen. *sec*-Butyllithium (Lithco) was obtained as a 1.3 M solution in cyclohexane and used without purification. Syringe and cannula techniques were used for all transfers. Carbon dioxide (Air Products, 99.995%) was used as received. (Tridecafluoro-1,1,2,2-tetrahydrooctyl)-1-dimethylchlorosilane (Huls) was degassed several times and vacuum distilled immediately prior to use (bp = 189–91 °C).

Polymerization and Functionalization. A stock supply of living lithium poly[(*sec*-butyl)-*b*-styrene-*b*-(styrene-d_8)] anion was prepared via sequential addition techniques using *sec*-butyllithium as the initiator in cyclohexane at 60 °C. A 10 000 number average molecular weight was calculated on the basis of the ratio of monomers to initiator, and for the purposes of this study, it was desirable to have a 75:25 weight percent ratio of styrene to styrene-d_8. An approximately equal volume of twice distilled tetrahydrofuran was added to the reactor containing the living block copolymer which had been cooled to room temperature.[15] This solution was quickly divided into three parts. Two parts were transferred to single-nicked round bottomed flasks that were previously fitted with rubber septa and Teflon stir bars and that had been flame dried under a nitrogen purge. The copolymer in the first round neck flask was terminated with an excess of degassed HPLC grade methanol to provide the hydrogen-terminated control material. A second, fluorosilane-terminated material was prepared by addition of the fluorinated chlorosilane into the second flask. The third, carboxylic acid end-functional polymer was prepared by directly terminating the third part of the original solution remaining in the reactor with ultrapure carbon dioxide.

The three polymers were isolated by precipitation into a mixture of methanol and 2-propanol, filtered, and dried in vacuo overnight at 60 °C. Molecular weight characterization results are given in Table 1, and the chemical structures are shown schematically in Figure 1. Titration of the carboxylic acid end groups confirms that the functionality was close to 1. XPS results[12] indicate the same to be true for the fluorosilane-terminated material. The percentage deuteration was measured using pyrolysis mass spectrometry by ratioing deuterated mass peaks to the total ion count, and also by ^{1}H NMR. These measurements indicated a percent deuteration of 22% rather than the anticipated 25% based upon the reaction stoichiometry. This was consistent with the NR results that provided contrast density values corresponding to a deuteration level of about 22%.

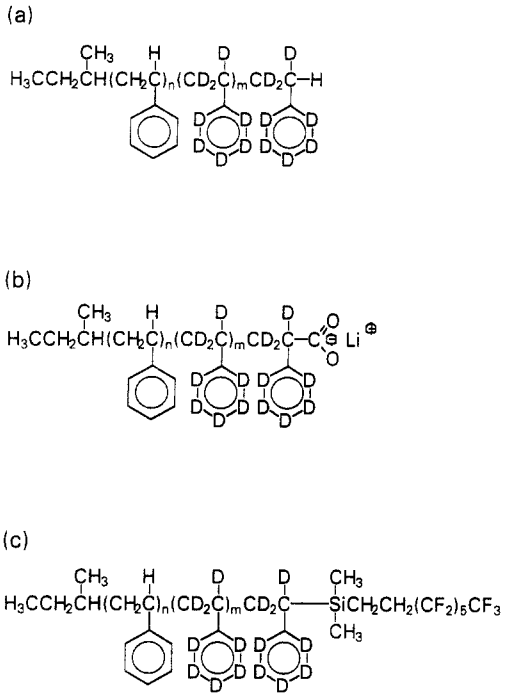

Figure 1. Schematic of polymer architectures ($n \approx 80$, $m \approx 19$): (a) "control" proton-terminated PS; (b) carboxy-terminated PS; (c) fluorosilane-terminated PS.

Film Preparation and Characterization. Filtered (Millipore Millex 0.2 μm) polymer solutions in toluene were spun cast onto 50 mm diameter, 5 mm thick substrates of either silicon (n type, 100) or fused silica that had been treated for 3 min using a Harrick plasma cleaner (Model PDC 236). This treatment typically yields a native silicon oxide layer of about 1.5–1.7 nm in the case of the silicon substrates. Spin casting conditions were adjusted to produce samples of two different thicknesses: approximately 40 and 100 nm. Sample equilibration was ensured by overnight annealing in air at 110 °C. This procedure was adopted in order to avoid potential surface contamination caused by a vacuum oven. X-ray photoelectron spectroscopy was applied to ensure that the thermal treatment did not cause any significant sample degradation. Oxygen concentrations were found to be negligible in the control film, ruling out the possibility of significant oxidation for these mild annealing conditions. Film thicknesses were then measured using a Rudolf Research AutoEL ellipsometer operating at 632.8 nm. The idential samples examined by ellipsometry were employed in the neutron reflection experiments. After the neutron reflection experiments, several of the samples were also measured with a J. A. Woollam Co. variable angle spectroscopic ellipsometer (VASE). The ellipsometric data indicated that the samples were relatively smooth, and XPS data did not indicate appreciable silicon signals, ruling out the possibility of film dewetting during the annealing procedures.

Neutron reflection data were obtained on the POSY II reflectometer at IPNS, Argonne National Laboratory.[16] The reflectivity curves are merged files from separate runs taken at different incident angles. The fitting program for the reflection data is an adaptation of software used for VASE from the J. A. Woollam Co. (Lincoln, NE).

XPS data were acquired on a Surface Science Instruments SSX-100 instrument equipped with a monochromatic aluminum source and operating at about 5×10^{-9} Torr. The electron takeoff angle was 35° with a cone of acceptance of ±12°, corresponding to a sampling depth of 3–4 nm. The sensitivity factors used for

Table 2. Parameters Employed in Neutron Reflection Modeling

sample	end group	nodes	layers	layer thickness (nm)
1	proton	16	112	0.4
2	proton	26	152	0.4; 28.2 (center layer)
3	fluorosilane	16	112	0.4
4	fluorosilane	16	112	0.4; 63.8 (center layer)
5	carboxy	16	112	0.4; 56.4 (center layer)

elemental quantification were those provided with the instrument software and verified with polymers of known stoichiometry (e.g., teflon).

Neutron Reflectivity Analysis. The reflection of neutrons from an interface is dependent upon the difference in refractive indices of the two media in contact.[17] For neutrons, the refractive index is given by

$$n = 1 - \frac{1}{2\pi}\lambda^2\frac{b}{v} \quad (1)$$

where λ is the wavelength and b/v is the scattering length density. In this study, we employ the method of isotopic deuterium substitution to label the chain backbone near the end group. The contrast of the perdeuterated polystyrene ($b/v = 6.3 \times 10^{-6}$ Å^{-2}) is considerably higher than that of the protonated polystyrene ($b/v = 1.43 \times 10^{-6}$ Å^{-2}).

The NR technique involves measuring the reflected beam intensity as a function of the momentum vector, $k = (4\pi/\lambda)\sin(\theta/2)$, where θ is the incident angle. Application of the technique has been discussed thoroughly in ref 17, so that we provide here only a few details of the procedures used for comparing the experimental curves to those generated from model contrast density profiles. The first step in fitting a particular end group concentration depth profile was to match the so-called Kiessig fringes in the NR data by the appropriate choice of overall film thickness. The thickness of the native silicon oxide layer was fixed at 1.6–1.7 nm on the basis of the ellipsometry measurements. It was noted that the error could be greatly reduced, particularly in the low k range, if the neutron scattering length density (b/v) for the silicon substrate was relaxed to about 2.01×10^{-6} Å^{-2}. This reduction in substrate b/v did not have a qualitative impact on profile shape, but did shift the whole polymer film part of the profile vertically. Having noted this phenomenon though, it was decided to constrain the b/v for the substrate to the literature value of 2.08×10^{-6} Å^{-2}. Models were allowed to relax from a starting homogeneous polymer layer with a b/v of 2.5×10^{-6} Å^{-2} (i.e., a polystyrene with about 22% deuteration). This layer was subdivided into many sublayers (thickness of ca. 0.4 nm, see Table 2) that were allowed to vary in b/v value. This should be considered quite conservative as it has been recommended that 2 nm slabs are sufficient to fit NR data.[17]

After the layered structure was created, a smaller number (see Table 2) of node positions were established. Between the node positions, the layer contrast was assumed to follow a linear gradient. Initially, many nodes at equally spaced positions were introduced, and their contrast was adjusted until the error was minimized. The contrast of all of the layers between the nodes also changes during this process since linear gradients are assumed between the nodes. After the initial minimization, the node positions were allowed to move in order to further reduce the error and converge on a global minimum. $\Delta k/k$ values (a measure of the reflectometer resolution) were initially set to 0.06 as a starting point and were subsequently allowed to float in order to minimize the overall error. The mean squared error (MSE) employed for this purpose is a normalized weighted sum of residuals defined as

$$\mathrm{MSE} = \sqrt{\frac{1}{N-M}\sum_{i=1,N}\left(\frac{R_{\mathrm{m},i} - R_{\mathrm{exp},i}}{s_i}\right)^2} \quad (2)$$

where N is the total number of data points, M is the number of fitting parameters, s_i is the standard deviation in the measured reflectivity, $R_{\mathrm{exp},i}$, and $R_{\mathrm{m},i}$ is the corresponding reflectivity calculated from the model density profile. Best fits gave $\Delta k/k$ values that ranged from 0.06 to 0.075 depending on the data set.

Table 3. Polystyrene Film Thicknesses on the Si Wafer

sample	end group	thickness (nm): NR	thickness (nm): ellipsometry
1	proton	43.3 + 1.6 (SiO_2)	43.5 + 1.6 (SiO_2)[a]
2	proton	105.6 + 1.7 (SiO_2)	105.3 + 1.6 (SiO_2)[a]
3	fluorosilane	43.2 + 1.7 (SiO_2)	46.0[b]
4	fluorosilane	106.2 + 1.7 (SiO_2)	106 + 1.7 (SiO_2)[a]
5	carboxy	103.7 + 1.7 (SiO_2)	105.6[b]

[a] Spectroscopic ellipsometry. [b] Single wavelength ellipsometry.

Results and Discussion

The NR technique furnishes a neutron scattering length density depth profile for the polymer–substrate layered specimen. In the present studies, the contrast is primarily provided by the higher b/v value of the deuterium labeled backbone (dPS) compared to that of the protonated polystyrene (hPS). Since the deuterium label is placed directly adjacent to the end group (see Figure 1), any localized enhancements of b/v values in the resultant profiles therefore reflect the location and spatial distribution of the end group.

The reflectivity profiles for the three end-functional materials are shown in Figures 4–8. Both thin (ca. 40 nm) and thick (ca. 100 nm) films were studied in order to document any possible effects due to the constraints imposed by the film thickness. The reflectivity curves show common features for all materials and are rich in complexity, suggesting that there is considerable structure in the films. The most prominent features evident in the profiles are the periodic intensity variations, the so-called Kiessig fringes, that result from interference of the reflections from the air–polymer and polymer–substrate interfaces. Analysis of the Kiessig fringes allows for determination of the total polymeric film thickness and the roughness of the two interfaces. Table 3 shows excellent agreement between the total film thicknesses as measured by ellipsometry and from the corresponding NR fits to the data (within <1% for VASE results).

The overall shape of the reflectivity profile, neglecting these Kiessig fringes, is related to the structure factor of the polymer film and contains information about the spatial distribution of the deuterium labels, and thus the distribution of the end groups. Some of the profiles, especially those in Figures 6–8, exhibit shapes with long wavelength oscillations, onto which are superimposed the periodic Kiessig fringes. These long wavelength oscillations indicate that the structure factor is periodic and consequently that the end group distribution with the thin polymer film is also periodic with a period smaller than that of the film thickness.

An advantage associated with the regression algorithm employed in this work is that a specific model for the end group distribution is not required in order to produce a model reflectivity curve. The algorithm self-adjusts the node positions and amplitudes in the model contrast density profile in working toward a minimum MSE. Since there exists no analytical function at present describing an anticipated end group density profile for our systems, a self-adjusting alorithm of this nature is a requirement if an unbiased fit is to be obtained. While this procedure never guarantees that a unique "best fit" is obtained, we have found that the algorithm converges to the same profile from a number of different starting conditions, leading us to believe that the results represent reasonable global minima.

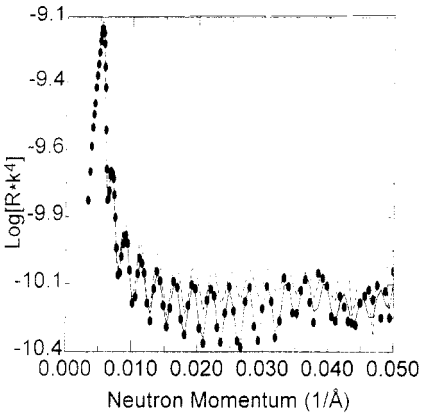

Figure 2. Reflectivity (Rk^4) curve (points) and model curves for the proton-terminated control sample (no. 2). The solid line is the best fit for an oscillatory end group profile, and the dashed line is the fit assuming a homogeneous end group distribution.

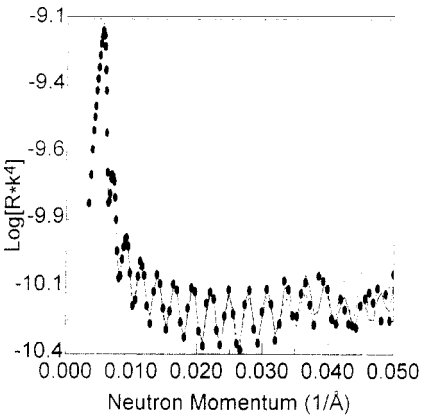

Figure 3. Reflectivity (Rk^4) curve (points) and model curves for the proton-terminated control sample (no. 2). The solid line is the best fit for an oscillatory end group profile, and the dashed line is the fit for a model assuming exponential end group (i.e., deuterium labeled end) depletion layers at both the air and substrate interfaces.

It is also possible to put bounds on the fitting process, such that any particular analytical model can be examined. This is useful in demonstrating the sensitivity of a given model to the fit parameters or in comparing different analytical profiles. In the present case, for example, we can examine the possibility that the end group distribution is homogeneous, such that the film corresponds to a single layer with constant contrast given by the stoichiometry. The comparison of the experimental and model reflectivity profiles, presented in Figure 2, clearly demonstrates that a homogeneous distribution of end groups does not describe the reflectivity curves. A second possibility to be examined is the presence of exponential composition gradients at the air and substrate interfaces, as have been employed in the previous study of the end group distribution.[14] A model of this nature produces a reflectivity curve that agrees fairly well with the experimental data, as shown in Figure 3. This model can be rejected, however, on the basis of physical grounds. The exponential profiles employed in the model profile are physically unrealistic, since a simple mass balance requires that the average contrast, integrated over one chain length, must be equal to the stoichiometric value. Therefore, end group composition profiles cannot be described by a simple exponential decay function as used in ref 14 but must be oscillatory in nature.[8] In addition, if we allow the exponential profile to self-adjust within the algorithm to minimize the error, oscillations always form, as the algorithm minimizes the error. The resultant best fit (Figure 3) corresponds better to the experimental data than does the exponential fit, and is also physically realistic. The improvement in correspondence with the data for the thick proton-terminated film (Figures 2 and 3) is also supported by the MSE values for the fits, which are 7.44, 3.00, and 2.64, respectively, for the flat, double exponential, and oscillatory profiles. The exponential profiles do not provide reasonable fits for the carboxylic and fluoro-terminated materials, while the best fit oscillatory profiles for these materials give acceptable MSE values of 3.42 and 3.26, respectively.

The remaining discussion will be based upon contrast density depth profiles that correspond to the minimum MSE values as described earlier, and thus can be considered "best fits". The lower parts of the figures show the b/v profiles corresponding to the best fit for each specimen. The calculated reflectivities for the model b/v profiles (solid lines) are compared with the reflectivity data (dashed lines) in the upper portion of the figures. The $\log[Rk^4]$ vs k plots employed in these figures amplify any differences between the model and experimental profiles. The model and data are almost indistinguishable in the figures, demonstrating that the reflectivity regression algorithm produces contrast depth profiles that are excellent representations of the data, without the need to generate a fixed mathematical model for the structure. The substrate is located at the left hand side of the contrast density profiles and provides two distinctive features: first there is a plateau at $b/v = 2.08 \times 10^{-6}$ Å^{-2} corresponding to the bulk silicon wafer; this is followed by a 1.61–1.7 nm thick layer of native silicon oxide with a constrast of about 3.5×10^{-6} Å^{-2}. The features to the right of the oxide layer reflect primarily the distribution of the deuterium labels in the polymer film. Since the label is adjacent to the end group, the high contrast in the density profile can be associated with the location of the end group of interest.

The results for the control (i.e., proton-terminated) samples demonstrate that there is a great deal of structure even for these "nonfunctional" materials. For both samples (Figures 4 and 5), the contrast density depth profiles exhibit pronounced oscillations at both the surface and the substrate; these dampen as the profile propagates into the interior of the film. Oscillations of this nature have been predicted for end-functional polymer melts[8] and are reminiscent of oscillatory concentration–depth profiles that have been predicted[13,18] and observed[19,20] for similar systems wherein one polymer chain contains two connected components (e.g., block copolymers). The b/v value at both interfaces corresponds to that of almost pure hPS, suggesting that the simple (deuterium labeled) protonated end group is repelled from both interfaces.

We had anticipated, on the basis of previous theoretical results,[13] that the simple control end group would be attracted to the surface. Consideration of the exact molecular structure of the chain (see Figure 1) provides the explanation as to why the opposite behavior is observed. The labeled polymers were all prepared by anionic synthesis techniques using *sec*-butyllithium as the initiator. The hPS and dPS chain segments therefore have different end groups: a *sec*-butyl group and a proton, respectively (see Figure 1a). The surface energy of the *sec*-butyl group can be approximated as that of a short hydrocarbon chain, on the order of 30 dyne/cm,[1] and is well below that of the polystyrene (39.4 dyne/cm at 20 °C for a similar molecular weight as used in this study[1]). Preferential adsorption of the lower surface energy *sec*-butyl group (and adjacent hPS sequence) at the air–polymer interface would thus be expected, on the basis of

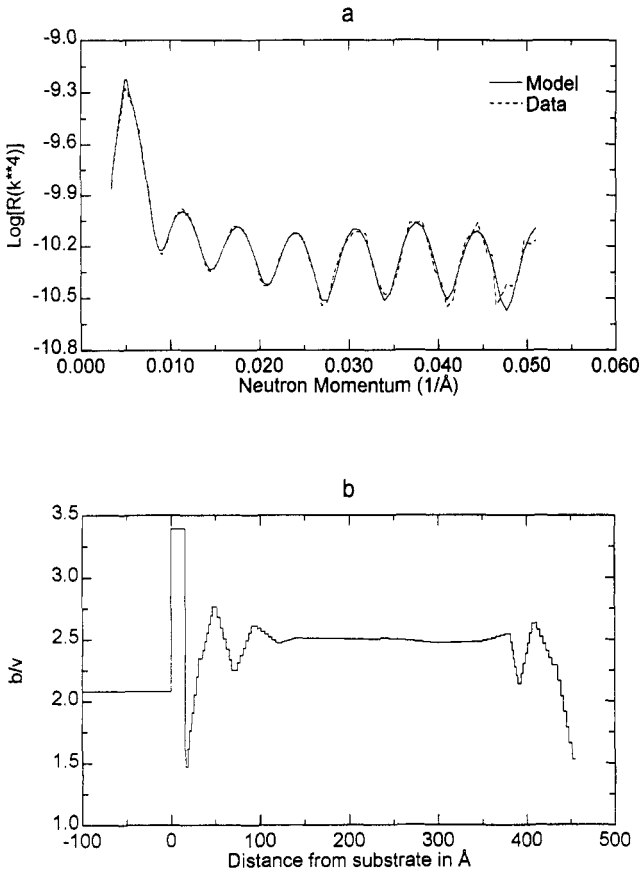

Figure 4. (a) Reflectivity (Rk^4) curve and model curve for the proton-terminated control sample (no. 1). (b) Optimal model contrast density depth profile.

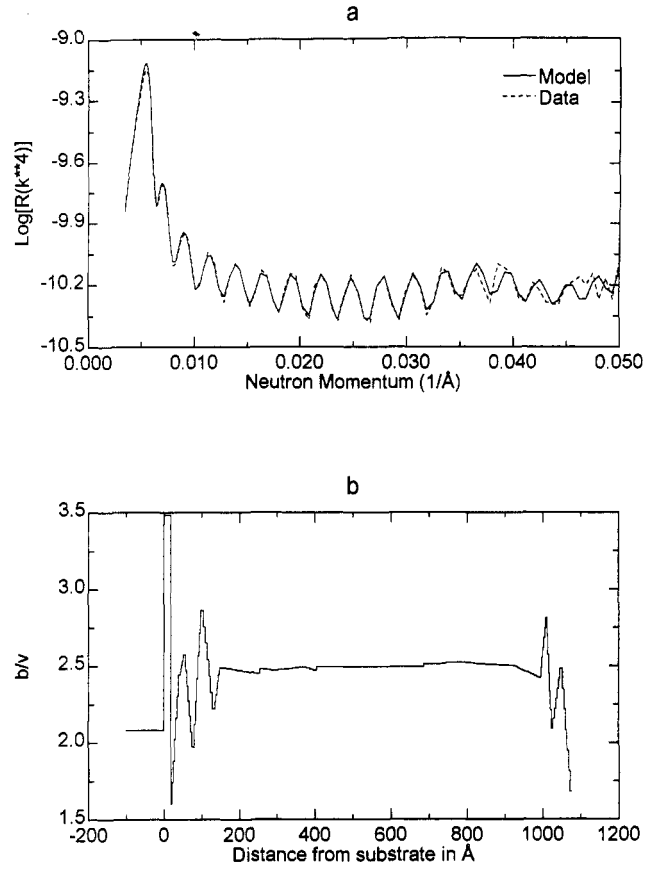

Figure 5. (a) Reflectivity (Rk^4) curve and model curve for the proton-terminated control sample (no. 2). (b) Optimal model contrast density depth profile.

the results of our lattice calculations,[8] and would dominate over adsorption of the other proton chain end. Preferential adsorption of the hPS chain end leads to the observed depletion of deuterium at the free surface since the perdeuterio and hydrogenous chain fragments are connected.

The contrast density profile at the substrate interface is also difficult to understand. The more polar polystyrene sequenes might be expected to interact more strongly with the native oxide on the substrate than will the low energy *sec*-butyl group. The data however suggest that either the *sec*-butyl group or perhaps the protonated polystyrene sequence prefers the substrate, as there is a depletion of contrast at the substrate interface. Similar behavior was found for poly(styrene-*b*-butadiene) copolymers, where the nonpolar butadiene block was found preferentially at the surface of a silicon wafer,[21] but this was observed for substrates stripped of the oxide layer. Studies on poly(styrene-*b*-methyl methacrylate) copolymers show that the more polar methyl methacrylate sequence is associated preferentially with a native oxide coated substrate,[22] and unpublished results for poly(styrene-*b*-isoprene) copolymers in the disordered state[23] show that the lower surface energy isoprene block adsorbs onto the native oxide. A recent article on the surface adsorption behavior of isotopic blends of polystyrene homopolymers[24] shows that the deuterated homopolymer adsorbs to the native oxide interface, at least for symmetric blends. It is not clear why the deuterium labeled portion of our diblock copolymer is not also absorbed in such fashion, and thus at present there appears to be no clear explanation for the behavior we observe at the substrate interface for the control sample.

The finding that the initiator fragment in anionic polystyrene can dominate the surface and interface properties of polystyrene is of great importance to the present studies, since all of the materials have *sec*-butyl groups as one chain terminus. The effects of the functional end group on the other chain terminus will therefore always be in competition with those of the initiator fragment. The effects of both end groups must be considered in concert and will complicate the interpretations we present for the distribution of the fluorosilane and carboxylic acid end groups.

The contrast density depth profiles for the fluorosilane-terminated samples (Figures 6 and 7) resemble those of the control samples at the wafer interface but are radically different at the surface. The contrast density at the surface attains a value of about 3.6×10^{-6} Å^{-2}, indicating a significant surface excess of deuterated chains due to adsorption of the adjacent fluorosilane end group. This results from the much lower surface energy (21.5 dyn/cm at 20 °C for low molecular weight PTFE[1]) of the fluorosilane end group compared to that of either hPS, dPS, or the *sec*-butyl terminus. Notice though that the b/v here is not that of pure dPS. The observed surface b/v value corresponds to a layer containing about 55% dPS segments. The actual percentage of dPS units at the surface cannot be determined since the volume and predominance of the fluorosilane end group (with b/v ca. 3×10^{-6} Å^{-2}) in this region also has an effect on the measured b/v. However recent HREELS (high resolution electron energy loss spectroscopy) measurements[25] of the percentage deuteration of the surface agree quite well with the corresponding NR value. Also notice that the b/v in the interior of the film is slightly less (2.48×10^{-6} Å^{-2} vs $(2.496\text{–}2.497) \times 10^{-6}$ Å^{-2}) than those of the other two materials. This reflects the dilution of dPS contrast by this large end group. A detailed angular dependent XPS study[12] of the fluorosilane-terminated polymer confirms

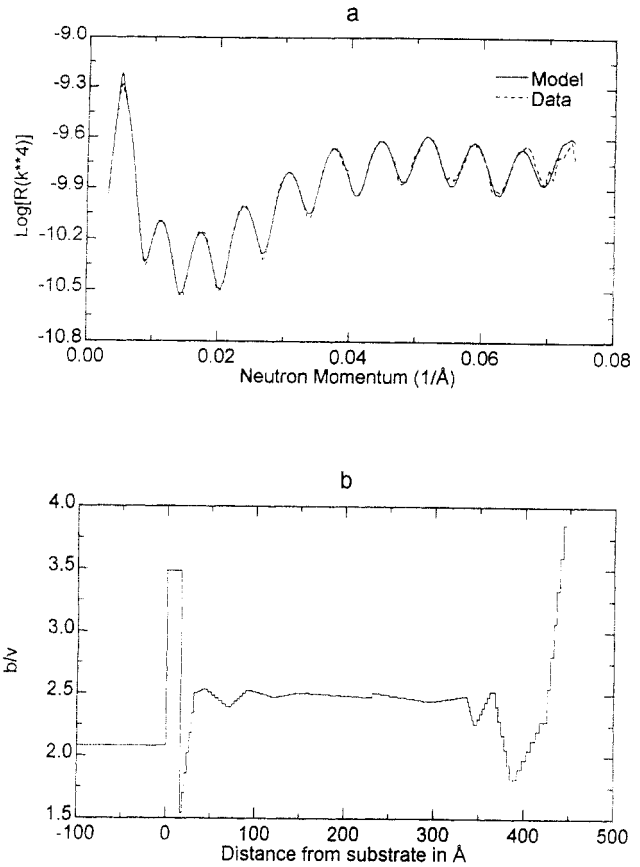

Figure 6. (a) Reflectivity (Rk^4) curve and model curve for the fluorosilane-terminated sample (no. 3). (b) Optimal model contrast density depth profile.

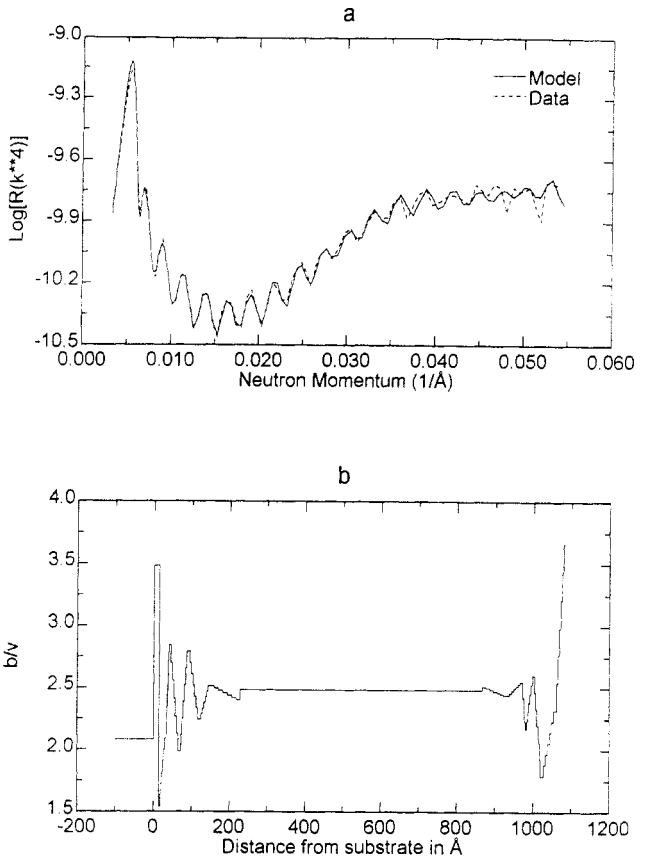

Figure 7. (a) Reflectivity (Rk^4) curve and model curve for the fluorosilane-terminated sample (no. 4). (b) Optimal model contrast density depth profile.

the oscillatory nature of the surface end group composition profiles determined by NR.

The fluorosilane group is clearly repelled from the high energy substrate, as indicated by the contrast depletion layer at the native oxide interface. This is consistent with the behavior we have observed when contacting the air–polymer interface with water.[26] We find that, in the presence of water, the fluorosilane end groups are repelled away from the interface in order to minimize their unfavorable contact with the highly polar water molecules. It appears that the oxide layer acts in a fashion here similar to that of the water in repelling the nonpolar fluorosilane end group.

The carboxy-terminated polymer (Figure 8) also shows an oscillatory contrast density depth profile with an enhanced concentration of dPS at the silicon oxide layer of the silicon wafer due to adsorption of the carboxyl end groups. The lack of strong attraction (only about 32% dPS at the wall) between the carboxy groups and the oxide layer may be attributable to the fact that about half of these end groups exist as carboxylate salts (perhaps as vestigial lithium carboxylates resulting from the use of a lithium initiator) as detected by FTIR. An earlier study,[21] however, stated that there was no observable difference in absorption behavior between OLi- and OH-terminated polystyrenes.

Contrast density depth profiles that had modest attraction *or* depletion of the carboxy end groups at the air–polymer interface were found to fit the reflectivity data equally well. The final profile selected shows a *depletion* of carboxy groups. This assignment was made on the basis of surface energy arguments that predict depletion of the high energy carboxy end groups,[8] and contact angle measurements that indicate that the surface behaves like a hydrophobic polystyrene backbone.[26] Complementary XPS measurements (Table 4) suggest there is surface enrichment of oxygen (1.1% oxygen compared to 0.2% expected from stoichiometry) that might be interpreted as an indication of carboxyl adsorption at the free surface; however adventitious oxygen is often found in XPS surface studies, and we believe that this result is not a contraindication to our hypothesis of carboxy depletion at the surface.

The contrast density depth profile for this polymer is also expected to be affected by the *sec*-butyl end group on one end of the chain. It is not clear from this result whether the actual surface gradient reflects repulsion of the carboxyl group, attraction of the *sec*-butyl group or a combination of both effects. The presence of both effects should lead to a concerted push–pull effect, leading to a strong segregation profile showing more relative segregation at the surface than that of the control sample. Experimentally, however, segregation is found to be weaker in the carboxy-terminated polymer, where b/v at the surface is about 1.85×10^{-6} Å^{-2}, compared to $(1.5–1.7) \times 10^{-6}$ Å^{-2} for the control samples. We believe that this difference may be attributed to the effects of water on the surface structure of the carboxy-terminated sample. Due to the experimental configuration for NR, it was not possible to keep the sample from contacting the atmosphere. When purposely contracted to water, the carboxy tipped PS shows an enhanced oxygen signal (8% O) as detected by XPS and a decrease in contact angle,[26,27] indicating that the surface structure can rearrange to allow the polar carboxy groups to contact the water, even at temperatures well below that of the bulk glass transition. The effects of a humid environment might then also provide an explanation for the behavior of the carboxy-terminated material.

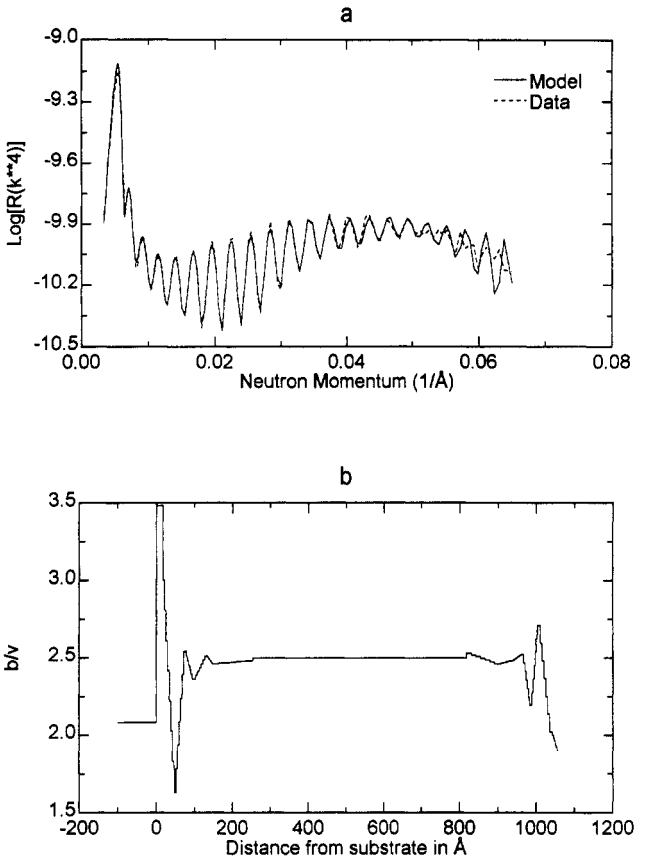

Figure 8. (a) Reflectivity (Rk^4) curve and model curve for the carboxy-terminated sample (no. 5). (b) Optimal model contrast density depth profile.

Table 4. XPS Atomic Surface Compositions after Postanneal (16 h in Air at 110 °C)[a]

sample	end group	% carbon	% oxygen	% fluorine	% silicon
1	proton	99.8 (100)	0.2 (0)	<0.1 (0)	<0.1 (0)
3	fluorosilane	94.5 (98.3)	0.5 (0)	4.8 (1.6)	0.2 (0.1)
5	carboxy	98.6 (99.8)	1.1 (0.2)	0.3 (0)	<0.1 (0)

[a] Bracketed values are based upon the known stoichiometry.

In previous studies of surface segregation effects for disordered block copolymers,[20] it was discovered that the film thickness strongly affected the surface segregation process for films with thicknesses on the order of 100 nm. The film thickness in the presnt study does influence the b/v profiles, but not to a large extent. If one compares composition profiles for the thick and thin versions of both the proton-terminated control and fluorosilane-terminated polymers, the b/v oscillations are more pronounced in the thicker films. In the previous study, thinner films were found to be more ordered, as a result of the influence of the surface energy on the bulk order–disorder transition. The opposite trend in the present case may be attributable to stronger packing constraints in thinner films of end-functional homopolymers. The end-functional polymers examined in this study are analogous to extremely asymmetric block copolymers, and thus it will be difficult for them to configure themselves into the lamellar concentration wave forced upon them by the surface segregation process. The additional material available in the thicker films may ease this constraint to a certain extent, leading to a more ordered structure.

XPS was performed on samples before NR analysis in order to ascertain whether the films' annealing procedure (16 h in air at 110 °C) introduced any unwanted oxidation. Table 4 shows the atomic surface compositions for the 43.3 nm thick proton-terminated film, the 43.2 nm thick fluorosilane-terminated film, and the 103.7 nm carboxy-terminated film. All XPS spectra show strong π to π^* transitions in the carbon 1s region, as would be expected for polystyrene. The proton-terminated material yields a clean spectrum corresponding to that expected for normal polystyrene. The carboxy-terminated polymer shows more surface oxygen than stoichiometry would predict (1.1% vs 0.2%) which can be attributed to a contaminant, minor oxidation, or preferential adsorption of the carboxy groups. Although we cannot completely rule out the latter possibility, contact angle measurements[26] do not indicate the existence of a polar surface, and we therefore believe that the excess oxygen may be attributed to adventitious oxygen from impurities, since no oxidation is indicated in the control specimen.

XPS analysis of the fluorosilane-terminated material shows an excess of surface fluorine (4.8%) as compared to the predicted stoichiometric amount (13 fluorines/834 total atoms = 1.6%), corroborating the interpretation of the NR and contact angle[26] results. The experimental atomic ratio of F to Si (F/Si = 24) reveals an excess of fluorine over the stoichiometric value (F/Si = 13), indicating that the signal from the silicon atoms is attenuated. This result suggests that the fluorinated portion of the end group must be oriented normal to the surface in order to shield the silicon atom. The carboxy-terminated polymer shows a slight (0.3%) fluorine contamination that may originate from the use of fluorocarbon containing filters prior to spin coating. Even if this 0.3% were taken into consideration to correct the data for the fluorosilane-terminated material, the F/Si ratio would equal 22, still well above the stoichiometric value.

The observed oscillations in the contrast density are due to the effects of chain connectivity. The end group concentration per chain is fixed by its architecture, such that a surface excess of an end group must necessarily be followed by a slightly deeper end group depletion layer. The local end group concentration integrated over one chain length must equal the average end group concentration for the material. End group concentration profiles consequently must always be oscillatory in nature if either the chain end or the chain backbone is preferentially adsorbed at a surface or interface. The existence of oscillatory end group concentration depth profiles has been predicted for confined homopolymer melts[13] and for end-functional homopolymers.[8]

Although our original intent was to provide a quantitative examination of end group distributions at the air–polymer interface, the nature of the conclusions we can make is limited by a number of experimental difficulties and unexpected effects. Our results indicate, for example, that surface adsorption of the initiator fragment should be expected in all cases where anionic polystyrenes are present at the air–polymer interface. The possibility of this behavior has been recognized in only one previous study of surface segragation behavior.[28] These authors demonstrated that the presence of the initiator fragment did not significantly affect the overall segregation behavior of isotopic polystyrene blends. These effects must be carefully considered, however, in any future surface studies of anionic polymers containing initiator fragments, as they add considerable complexity to the task of interpreting NR profiles. In further studies of end group distribution at polymer interfaces, it would be desirable to use an anionic initiator that does not leave a residue at the chain end.

A second effect that influences our results is the use of a relatively long deuterium sequence to tag the end group.

Table 5. Periodic Repeat Distances for End Group Concentration Profiles at the Substrate Interface

specimen	end group	distance from substrate to maxima and minima (nm) 1st	2nd	3rd	4th	5th	av half-layer thickness (nm)
1	proton	3.2	5.5	7.8	10.4		2.7
2	proton	3.1	6.1	8.4	11.4		2.9
3	fluorosilane	2.6	5.4	7.4			2.6
4	fluorosilane	2.8	5.2	7.2	10.2	13.7	2.6
5	carboxy	3.1	4.8	8.4	11.4		2.8

Table 6. Periodic Repeat Distances for End Group Concentration Profiles at the Air–Polymer Interface

specimen	end group	distance from substrate to maxima and minima (nm) 1st	2nd	3rd	av half-layer thickness (nm)
1	proton	4.1	5.9	7.4	2.9
2	proton	2.7	5.1	6.6	2.4
3	fluorosilane	6.2	8.5	10.5	4.2
4	fluorosilane	5.7	7.9	9.9	3.9
5	carboxy	3.8	6.8	9.2	3.3

While a large concentration of the label was chosen to increase the NR signal, it also smears out the concentration depth profile, since the deuterium distribution may be broader than the true end group distribution. The use of deuterium labeling itself may add additional complexity, due to the possibility that one of the isotopes may preferentially adsorb at either the native oxide[24] or air–polymer[29–32] interfaces. In our case, however, these isotopic effects are dominated by those of the end groups, since their influence on surface energy is much smaller than that of the end groups. Finally, there are some minor limitations associated with the modeling approach that we have adopted. In the present case, the concentration profiles between nodes are assumed to be linear in nature, leading to profiles that are not entirely smooth, as would be the true profile. The complexity of the concentration profiles and precision of the data however do not warrant more extensive modeling since the agreement between the model calculations and the data is already exceptionally good.

The most reliable parameter that can be extracted from the analysis is the period of the end group concentration wave that propagates from the surface. The values for the periods of these oscillations are listed in Tables 5 and 6. These can be compared to the unperturbed dimensions for a polystyrene of similar molecular weight. Using a literature correlation for the radius of gyration of polystyrene in a Θ solvent,[33] we calculate a radius of gyration of about 2.9 nm for 10 300 molecular weight polystyrene. Looking first at Table 5, one sees the distances of both the minima and maxima in the concentration depth profile measured from the substrate interface. The average distance between adjacent minima and maxima is in the range 2.6–2.9 nm, close to the predicted radius of gyration, and is not, within the errors of the fitting procedure, dependent on the end group type.

The corresponding data describing the structure at the air–polymer interface are shown in Table 6. Here there appears to be some dependence on the end group type. The control samples give values of the average half-layer thickness again in the range 2.4–2.9 nm, as found for the substrate data. The half-layer thicknesses of the fluorosilane-terminated polymer, however, are much larger, in the range 3.9–4.2 nm. The first half-layer for these films is even thicker, in the range 5.7–6.2 nm. As discussed earlier, the XPS data suggest that the fluorosilane end groups are partially oriented normal to the surface. The size of this end group is nonnegligible and must be included in the calculation of the half-layer thickness. If we assume that the polystyrene portion of the chain is configured in a fashion similar to that in the control sample (with an average thickness of the first half-layer equal to 3.4 nm), we calculate that the fluorosilane end group must accout for another 2.6 nm. The extended chain length of the fluorosilane, however, is on the order of only 1.2 nm. The polymer backbone therefore must be partially extended to account for the larger half-layer thickness in this material.

The behavior of the fluorosilane-terminated polymer is reminiscent of that of lamellar copolymers. It is well-known in these materials that the block of lower surface energy adsorbs preferentially at the surface[34] and that the chains adopt extended configurations in order to pack in the lamellar geometry.[35,36] The ordering in this material does not propagate throughout the entire film as it would if the material were microphase separated, so that the behavior is more analogous to that of surface induced ordering of a disordered block copolymer.[19,20] The theory for the latter systems[18] predicts a damped cosine function for the surface concentration gradient, similar to what we observe for the fluorosilane-terminated polymer film, but our end block (i.e., the end group) is too short to be properly treated by the theory (valid for symmetric copolymers). The overall surface induced ordering behavior of our end-functional polymers can be considered, however, qualitatively consistent with what is predicted and observed for disordered block copolymers. We do not observe discrete Bragg peaks due to these oscillations, as have been observed for some of the block copolymer studies;[19] however it was also shown[20] that the Bragg peaks for copolymers broaden considerably at temperatures well above the order–disorder temperature, and our systems are well removed from any such transition.

Summary

Neutron reflectivity and X-ray photoelectron spectroscopy are applied to characterize the segregation of the chain termini to both the native oxide on a silicon substrate and the air–polymer interface. Functional polystyrene homopolymers are examined, each containing a short perdeuteriostyrene sequence adjacent to the chain end. Three different chain ends are considered: a proton (neutral end group), a carboxylic acid (repulsive to the surface), and a fluorosilane (attractive to the surface). In the proton-terminated control material, the butyllithium initiator fragment is found to adsorb at both interfaces. The carboxy terminus adsorbs to the native oxide interface but is repelled from the air–polymer interface, while the fluorosilane terminus is repelled from the native oxide interface but is attracted to the air–polymer interface. The apparent end group concentration depth profiles (i.e., neutron contrast profiles) for all three polymers are periodic in nature at both interfaces, with the amplitude of the concentration fluctuations damping out with increasing depth. This behavior is expected due to the connectivity of the chain end and backbone. The periodicity of the oscillations is on the order of the unperturbed polymer chain dimensions, with the exception of the fluorosilane-terminated polymer, where the periods are larger, indicating that the polymer backbone is extended near the air–polymer interface.

Acknowledgment. This research was supported in part by grants from the Army Research Office and the National Science Foundation Polymers Program of the

Division of Materials Research (No. DMR-8818232). The authors would like to thank Sally Miller, Tom Mourey, Patty Christiano, and Phil Keogh (Analytical Technology Division, Eastman Kodak Co.) for the SEC and pyrolysis MS analyses.

References and Notes

(1) Wu, S. *Polymer Interface and Adhesion*; Marcel Dekker: New York, 1982.
(2) Pan, D. H.; Prest, M. W., Jr. *J. Appl. Phys.* **1985**, *58*, 15.
(3) Bhatia, Q. S.; Pan D. H.; Koberstein, J. T. *Macromolecules* **1988**, *21*, 2166.
(4) Ober, R.; Paz, L.; Taupin, C.; Pincus, P.; Boileau, S. *Macromolecules* **1983**, *16*, 50.
(5) Rastogi, A. K.; St. Pierre, L. E. *J. Colloid Interface Sci.* **1969**, *31*, 168.
(6) Schmidt, I.; Binder, K. *J. Phys. (Paris)* **1985**, *46*, 1631.
(7) Jalbert, C.; Koberstein, J. T.; Yilgor, I.; Gallagher, P.; Krukonis, V. *Macromolecules* **1993**, *26*, 3069.
(8) Jalbert, C.; Koberstein, J. T.; Kumar, S.; Hariharan, A. Manuscript in preparation.
(9) Jalbert, C.; Koberstein, J. T.; Balaji, R.; Bhatia, Q.; Salvati, L.; Yilgor I. *Macromolecules* **1994**, *27*, 2409.
(10) Fleischer, C. A.; Koberstein, J. T.; Krukonis, V.; Wetmore, P. *Macromolecules* **1993**, *26*, 4172.
(11) Fleischer, C. A.; Morales, A. R.; Koberstein, J. T. *Macromolecules* **1994**, *27*, 379.
(12) Jalbert, C.; Elman, J. F.; Long, T. E.; Koberstein, J. T. Manuscript in preparation.
(13) Kumar, S. K.; Vacatello, M.; Yoon, D. Y. *Macromolecules* **1990**, *23*, 2189.
(14) Zhao, W.; Zhao, X.; Rafailovich, M. H.; Sokolov, J.; Composto, R. J.; Smith, S. D.; Satkowski, M.; Russell, T. P.; Dozier, W. D.; Mansfield, T. *Macromolecules* **1993**, *26*, 561.
(15) Quirk, R. P.; Yin, J.; Fetters, L. J.; Kastrup, R. V. *Macromolecules* **1992**, *25*, 2262.
(16) Felcher, G. P.; Hilleke, R. O.; Crawford, R. K.; Haumann, J.; Kleb, R.; Ostrowski, G. *Rev. Sci. Instrum.* **1987**, *58*, 609.
(17) Russell, T. P. *Mater. Sci. Rep.* **1990**, *5*, 171.
(18) Fredrickson, G. H. *Macromolecules* **1987**, *20*, 2535.
(19) Anastasiadis, S. H.; Russell, T. P.; Satija, S. K.; Majkrzak, C. F. *Phy. Rev. Lett.* **1989**, *62* (16), 1852.
(20) Menelle, A.; Russell, T. P.; Anastasiadis, S. H.; Satija, S. K.; Majkrzak, C. F. *Phys. Rev. Lett.* **1992**, *68* (1), 67.
(21) Jones, R. A. L.; Norton, L. J.; Shull, K. R.; Kramer, E. J.; Felcher, G. P.; Karim, A.; Fetters, L. J. *Macromolecules* **1992**, *25*, 2359.
(22) Green, P. F.; Christensen, T. M.; Russell, T. P.; Jerome, R. *Macromolecules* **1989**, *22*, 2189.
(23) S. H. Anastasiadis, private communication.
(24) Hariharan, A.; Kumar, S.; Rafailovich, M. H.; Sokolov, J.; Zheng, X.; Duong, D.; Schwarz, S. A.; Russell, T. P. *J. Chem. Phys.* **1993**, *99* (1), 656.
(25) Elman, J. F.; Apai, G. R.; McKenna, W. P.; Long, T. E.; Koberstein, J. T. Presented at the American Vacuum Society National Meeting, Orlando, FL, November 1993; manuscript in preparation.
(26) Jalbert, C. Ph.D. Dissertation, University of Connecticut, Storrs, CT, 1993.
(27) Elman, J. F. Unpublished data.
(28) Hariharan, A.; Kumar, S. K.; Russell, T. P. *J. Chem. Phys.* **1993**, *98* (5), 4163.
(29) Hariharan, A.; Kumar, S. K.; Russell, T. P. *J. Chem. Phys.* **1993**, *99* (5), 4041.
(30) Russell, T. P.; Karim, A.; Mansour, A.; Felcher, G. P. *Macromolecules* **1988**, *21*, 1890.
(31) Zhao, X.; Zhao, W.; Sokolov, J.; Rafailovich, M. H.; Schwarz, S. A.; Wilkens, B. J.; Jones, R. A. L.; Kramer, E. J. *Macromolecules* **1991**, *24*, 5991.
(32) Jones, R. A. L.; Norton, L. J.; Kramer, E. J.; Composto, R. J.; Stein, R. S.; Russell, T. P.; Mansour, A.; Karim, A.; Felcher, G. P.; Rafailovich, M. H.; Sokolov, J.; Zhao, X.; Schwarz, S. S. *Europhys. Lett.* **1990**, *12*, 41.
(33) *Polymer Handbook*, 3rd ed.; Brandup, J., Immergut, E. H., Eds.; John Wiley and Sons: New York, 1989. Calculated from the expression $SM^{-1/2} = 0.0288$, where S is the radius of gyration in nanometers and M is the molecular weight.
(34) Dwight, D. W.; McGrath, J. E.; Riffle, J. S.; Smith, S. D.; York, G. A. *J. Electron Spectrosc. Relat. Phenom.* **1990**, *52*, 457.
(35) Matsushita, Y.; Mori, K.; Mogi, Y.; Saguchi, R.; Noda, I.; Nagasawa, M.; Chang, T.; Glinka, C. J.; Han, C. C. *Macromolecules* **1990**, *23*, 4317.
(36) Quan, X.; Gancarz, I.; Koberstein, J. T.; Wignall, G. D. *J. Polym. Sci., Polym. Phys. Ed.* **1987**, *25*, 641.